ACS Sustainable Chemistry & Engineering

Research Article

pubs.acs.org/journal/ascecg

Morphology and Thermal Properties of Renewable Resource-Based Polymer Blend Nanocomposites Influenced by a Reactive Compatibilizer

P. J. Jandas, S. Mohanty,* and S. K. Nayak

Laboratory for Advanced Research in Polymeric Materials (LARPM) Central Institute of Plastics Engineering and Technology (CIPET), Bhubenaswer, India 751024

ABSTRACT: Partially miscible blends of poly(lactic acid) (PLA) and poly(hydroxybutyrate) (PHB) have been prepared by the melt mixing method. An interpenetrating network structure created by a maleic anhydride (MA) compatibilizer imparted additional interactions between the two matrices, which has resulted in increased miscibility within the blends. A modified interface has been characterized using morphological analysis through FT-IR and SEM analysis. Because MA compatibilization distributed flexible intermolecular hydrogen bonding within the blend matrix, elongation at break and Izod impact strength has been reported at a maximum of 540.17% and 99%, respectively, compared to those of the PLA matrix. Further, incorporation of layered silicates within the optimized composition of the PLA/PHB/MA blend modified the tensile strength by 49%, without compromising its superior flexible characteristics. Simultaneously, the renowned thermal insulating property of exfoliated/intercalated layered silicate works well to promote the thermal stability of the blend as well. Because two different nanoclays have been utilized in the present investigation, a comparative account of the extent of the intercalation/exfoliation has been reported through morphological analysis.

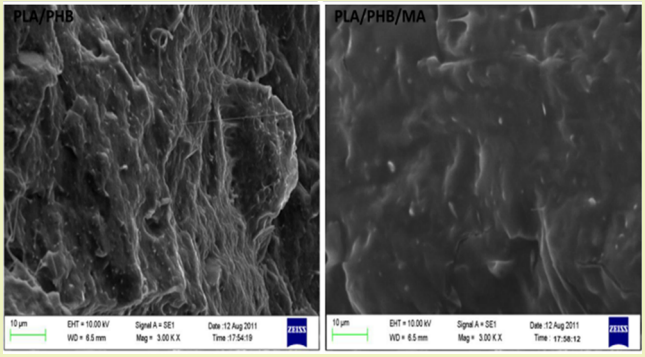

KEYWORDS: *PLA, PHB, Blend nanocomposites, OMMT*

INTRODUCTION

Poly(lactic acid) (PLA) is one of the most promising biodegradable polymers with comparable/better performance characteristics than that of synthetic commodity plastics. However, its brittle nature has to be modified to ensure its potentiality as a substitute for petroleum-based materials. Several studies are available in this area by suggesting modification methods for PLA to convert it as a commodity material.[1] Major experimentations have been conducted on the toughness of PLA through plasticization, copolymerization, and melt blending with soft polymers.[2]

Properties of polymer blends generally depend upon the thermodynamic miscibility between the individual polymers. Polymer products containing biodegradable components are of great interest because of the way in which their properties and biodegradation characteristics can be tailored.[3] PLA and PHB are biodegradable polyesters with comparable physical properties and miscibility constants.[4] PLA/PHB blends prepared through the melt blending method have been reported by Zhang et al.[5] The authors suggested partial miscibility within the blends that requires interfacial compatibilization to achieve the properties as per the expected level. The present investigation has tried to enhance the ductility nature of PLA by melt blending with poly(hydroxybutyrate) (PHB) and the reactive compatibilizer maleic anhydride (MA). MA can induce flexible physical interactions like dipole−dipole or hydrogen bonding that can contribute additional miscibility as well as additional flexibility to the blend matrix. Further, organically modified nanoclays, OMMT and C30B, were exfoliated/intercalated within the compatibilized blend matrix to compensate the drawbacks resulting from the blending process. Miscibility of the blend has been evaluated using morphological and DSC analysis. In addition, mechanical, dynamic mechanical, and thermal characteristics have also been studied.

EXPERIMENTAL SECTION

Materials. PLA (Grade 4042D) with a density of 1.24 g/cm^3 (M_w = 211,332 g/mol and M_w/M_n = 2) and L-lactide and D-lactide ratio 92:8 were purchased from NatureWorks, U.S.A. PHB (Grade P226) with a density of 1.25 g/cm^3 (M_w = 426, 000 g/mol) was purchased from Biomer, Germany. Natural montmorillonite (NaMMT) and commercially modified montmorillonite Cloisite 30B [(C30B) with a modifier MT2EtOT: methyl tallow bis-2-hydroxy ethyl quaternary ammonium salt and CEC of 90 meq/100g clay] were obtained from Southern Clay Products, U.S.A. Compatibilizer (MA), initiator, benzoil peroxide (BPO), and a surface modifier for nanoclay, Hexadecyltrimethyl ammonium bromide (HTAB), have been procured from Sigma Aldrich Co., Germany, and used without any modification.

Received: May 23, 2013
Revised: December 3, 2013
Published: December 10, 2013

Table 1. Mechanical Properties of PLA, PHB, Blends, and Its Blend Nanocomposites

sample	tensile modulus (MPa)	tensile strength (MPa)	elongation at break (%)	impact strength (J/m)
V-PLA	3550.21 ± 36.61	38.55 ± 5.33	2.91 ± 0.32	25.70 ± 2.30
V-PHB	2611.34 ± 42.53	27.56 ± 9.53	3.32 ± 1.21	28.22 ± 4.55
PLA/PHB (90/10)	3502.72 ± 66.76	37.73 ± 7.65	5.53 ± 3.11	23.53 ± 7.51
PLA/PHB (80/20)	3445.52 ± 81.41	35.14 ± 9.22	8.17 ± 3.52	25.30 ± 8.63
PLA/PHB (70/30)	3388.13 ± 64.39	34.64 ± 7.31	12.41 ± 3.32	29.53 ± 4.72
PLA/PHB (60/40)	2702.83 ± 82.52	23.75 ± 9.41	8.94 ± 4.74	14.47 ± 5.28
PLA/PHB/MA (70/30/1)	3344.91 ± 45.27	29.51 ± 9.34	31.73 ± 8.56	24.04 ± 6.62
PLA/PHB/MA (70/30/3)	3326.93 ± 67.36	25.54 ± 5.54	48.89 ± 5.72	24.55 ± 7.28
PLA/PHB/MA (70/30/5)	3015.67 ± 54.45	25.43 ± 9.56	365.45 ± 11.66	42.73 ± 5.99
PLA/PHB/MA (70/30/7)	3020.75 ± 49.19	22.55 ± 9.39	540.17 ± 32.82	49.21 ± 3.62
PLA/PHB/MA (70/30/9)	3018.53 ± 71.25	15.23 ± 4.48	448.39 ± 46.52	50.94 ± 6.52
PLA/PHB/MA/C30B (70/30/7/1)	4107.82 ± 76.52	33.55 ± 9.23	503.13 ± 43.24	45.73 ± 2.30
PLA/PHB/MA/C30B (70/30/7/3)	4222.64 ± 55.27	43.64 ± 6.53	488.24 ± 45.86	57.74 ± 9.44
PLA/PHB/MA/C30B (70/30/7/5)	3976.93 ± 98.34	25.86 ± 8.52	376.88 ± 41.42	52.82 ± 6.45
PLA/PHB/MA/OMMT (70/30/7/1)	4167.75 ± 85.39	37.17 ± 3.52	456.71 ± 65.73	44.25 ± 9.31
PLA/PHB/MA/OMMT (70/30/7/3)	4332.56 ± 43.43	48.23 ± 5.59	457.84 ± 12.49	59.65 ± 8.48
PLA/PHB/MA/OMMT (70/30/7/5)	3423.97 ± 23.41	19.62 ± 5.96	312.96 ± 23.65	56.86 ± 9.62

Methods. *Surface Modification of NaMMT.* Surface modification of NaMMT has been conducted as per our previous study.[6] Ten grams of NaMMT was dispersed in 300 mL of distilled water using a mechanical stirrer. Further HTAB surfactant (0.1 molar solutions in distilled water) acidified with 2 mL of HCl was added to the nanoclay dispersion. The mixture was stirred for 2 h, followed by centrifugation and filtration until complete removal of the bromide group from the filtrate. Residual bromide was detected using the $AgNO_3$ test. The filtered organically modified nanoclay (OMMT) was dried at 80 °C for 12 h and milled under cryogenic conditions.

Preparation of Blends and Blend Nanocomposites. Prior to compounding, PLA and PHB were predried at 80 °C in a vacuum oven for 12 h. Subsequently, the blends have been prepared in a co-rotating twin-screw mini-extruder (DSM Xplore 15, The Netherlands) attached with mini-injection molder. Various wt % of PHB ranging from 10 to 40 have been incorporated into the PLA matrix. Processing temperatures have been optimized at 170, 175, and 180 °C for the three successive zones of the extruder with a screw speed of 40 rpm (acceleration rate: 50 rpm/min). Melt has been collected from the extruder, and test samples have been prepared using an injection molder according to respective ASTM standards. Injection molding parameters were fixed at a mold temperature of 40 °C, melt temperature of 170 °C, injection time of 5 s, and injection pressure of 10 bar. Further, the compatibilzer and nanoclays (C30B and OMMT) have been incorporated to the optimized composition of blends under the above-mentioned processing parameters for preparing compatibilized blend nanocomposites. BPO has been used as an initiator for MA compatibilization with an amount less than 0.5% of MA used in each cases.

Characterization. *Mechanical Testing.* The tensile measurements of V-PLA, V-PHB, blends, and blend nanocomposites were carried out in a universal testing machine (Instron 3386, U.K.). In all the cases, dumbbell-shaped specimens with dimensions of 165 mm × 12.7 mm × 3 mm as per ASTM D 638 have been used. Gauge length was kept fixed at 50 mm with a cross head of 5 mm/min for conducting the test. Specimens with dimensions of 63.5 mm × 12.7 mm × 3 mm were used for measurement in the Izod impact test using an Impactometer (Ceast, Italy) as per ASTM D 256. The specimens were notched at angle of 45° and a depth of 2.54 mm using a notch cutter (Ceast, Italy) prior to test. For all the tests including tensile and Izod impact, five samples of each composition have been tested.

Morphological Analysis. Miscibility of the blends was evaluated using FT-IR spectroscopy with a FT-IR spectrometer, Nicolet 6700, U.S.A. Spectra were obtained at 4 cm^{-1} resolution and number of scan 64 in the standard wavenumber range from 400 to 4000 cm^{-1}. All the samples have been dried under vacuum at 60 °C for 12 h before testing. Further, the interface of the blends also has been studied through SEM analysis using a Zeiss EVO-MA, U.K., instrument. The samples were coated with gold using a vacuum sputter coater prior to testing to improve the surface conductivity.

Wide angle X-ray diffraction (WAXD) analysis was performed for blend nanocomposites to study the extent of intercalation/exfoliation of nanoclays within the polymer matrix using a Schimadzu X-ray diffractometer 7000L, Japan, (graphite monochromator Cu $K\infty_1$ radiation with λ = 0.15406 nm) at a scanning rate of 0.5°/min within a range from 1° to 50°. The basal spacing of the silicate layer, d, was calculated using the Bragg's equation, $\lambda = 2d \sin \theta$.

TEM images of blend nanocomposites were used with a transmission electron microscope, JEM 1400 TEM mode, JEOL, Japan. Samples for imaging were prepared by slicing the sample to an ultrathin size of less than 100 nm using a Cryo Leica EM-UC6 instrument (Leica Microsystems, Switzerland) with a diamond knife, and it was viewed without staining.

Thermal Analysis. Thermal transitions of blends and blend nanocomposites were studied in comparison with the virgin matrices using differential scanning calorimetry (DSC, Q20, TA Instruments, U.S.A.). A sample of ≤7 mg was heated from room temperature to 180 °C, held for 5 min to remove the previous thermal history, cooled to −50 °C at a rate 10 °C/min, and reheated again to 180 °C with the same rate under N_2 atmosphere. The corresponding melting (T_m), cold crystallization (T_{cc}), heat of fusion (ΔH_m), and degree of crystallinity were noted.

Thermal stability of the samples was evaluated using a thermogravimetric analyzer (TGA, Q50, TA Instruments, U.S.A.). Samples of about 7 mg were heated from 50 to 600 °C at a rate of 10 °C/min under N_2 flow (60 mL/min). Corresponding weight loss against temperature was noted.

Dynamic Mechanical Analysis (DMA). Dynamic mechanical analyzer (DMA, Q800, TA Instruments, U.S.A.) was employed for measuring viscoelastic properties of the samples as a function blending, compatibilization, and blend nanocomposite preparation. Samples with dimensions of 63.5 mm × 12.7 mm × 3 mm were used for testing under a temperature range of 40−150 °C and a fixed frequency of 1 Hz.

RESULTS AND DISCUSSION

Mechanical Properties. *Mechanical Properties of PLA/PHB Blends with variable PHB Loading.* Mechanical properties of virgin PLA (V-PLA), virgin PHB (V-PHB), and their blends with different ratios are depicted in Table 1. V-PLA has a reported tensile strength of 38.55 MPa, tensile modulus of 3550.21 MPa, and impact strength of 25.70 J/m. Incorporation of PHB within the PLA matrix results in intermediate

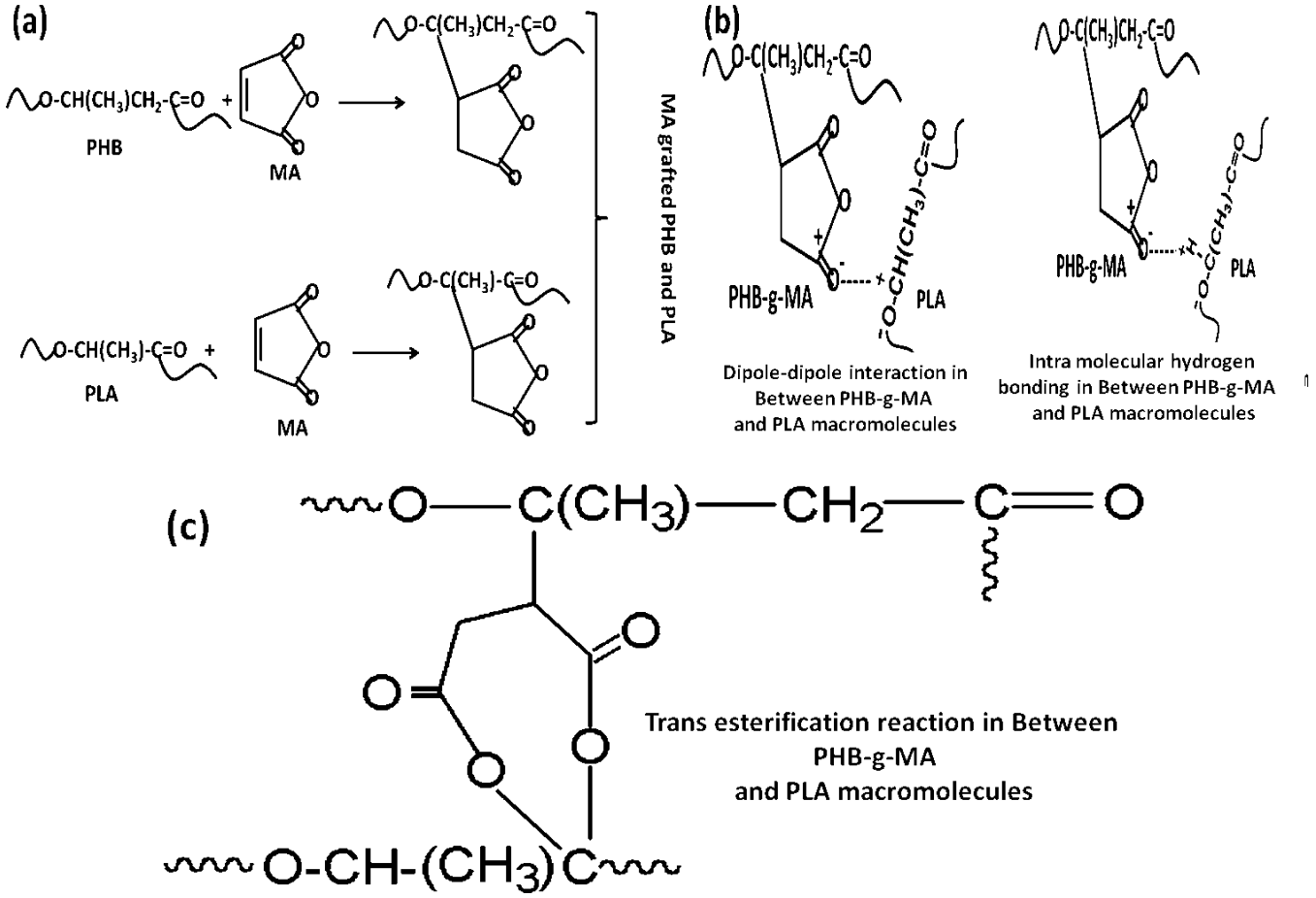

Figure 1. (a) Scheme for reactive compatibilization of PLA/PHB using MA. (b) Interacting pattern for MA grafted PLA and PHB with other macromolecules. (c) Transesterification reaction between PLA and PHB-g-MA.

properties for the blends. However, the ductility of V-PLA increased consistently with an increase in PHB concentration from 10 to 30 wt % within the PLA matrix. The blend prepared at a 70:30 ratio of PLA:PHB showed an optimum increase in percentage elongation of 76.55%. The observation suggests some degree of molecular interaction between the macromolecules of PLA and PHB within the blend. Finely dispersed PHB crystals act like a reinforcing filler within the PLA matrix, which has a polar C═O group, inducing a molecular interaction through dipole−dipole or intermolecular hydrogen bonding within the blend matrix. Izod impact strength was also increased consistently up to 29.5 J/m with the 30% PHB loading. Enhanced ductility provides better energy absorbing capability to the PLA matrix as a result of a change in the mechanical deformation process either through the promotion of extensive shear yielding or craze formation or a combination of both.

However, the tensile modulus and tensile strength of PLA were shown to considerably decrease in the case of PLA/PHB blends. Increased ductility and flexibility tend to reduce the stiffness of the matrix and may be the reason for this depression. Partial rearrangement of rigid cohesive bonds also tends to distort the crystalline pattern of the PLA matrix as well as the total crystallinity of the system. As a result, a corresponding decrease in stiffness has been observed after PHB incorporation. Because the blend prepared at a 70:30 (PLA:PHB) ratio exhibits optimum elongation at break and impact strength, the composition has been used for trial with a compatibilizer and preparation of blend nanocomposites.[7]

Effect of Compatibizer on Mechanical Properties of PLA/PHB Blends. According to the Hildebrand solubility theory, a large difference in solubility parameters (δp) of individual matrices results in the immiscible blend in the absence of any interfacial compatibilizer.[8] PLA and PHB have Hildebrand solubility parameters (δp) of 23.5 and 19.8 J/cm, which points to partial miscibility between the two polymers. Reactive extrusion with maleic anhydride (MA) has been a well-established technique for the compatibilization of polymer blends. The compatibilization technique follows the grafting mechanism of MA on the α-carbon atom of the carbonyl group in the PLA and PHB macromolecules as depicted in Figure 1(a). Grafted MA pendant facilitates improved interaction among the macromolecular chains of PLA and PHB. The proposed interaction between MA and the macromolecules of PLA or PHB is depicted in Figure 1(b,c). MA acts like a bridging unit between the polar molecular strands of PLA and PHB through covalent bonds by a transesterification reaction and dipole−dipole and intermolecular hydrogen bonding, which results in improved interaction between the two polymers. This increased interaction results in better miscibility within the blend as a function of MA compatibilization. As a result, fracture behavior of the specimen during the tensile test changed from a brittle characteristic of V-PLA to a ductile fracture of PLA/PHB/MA blends. The elongation at break of

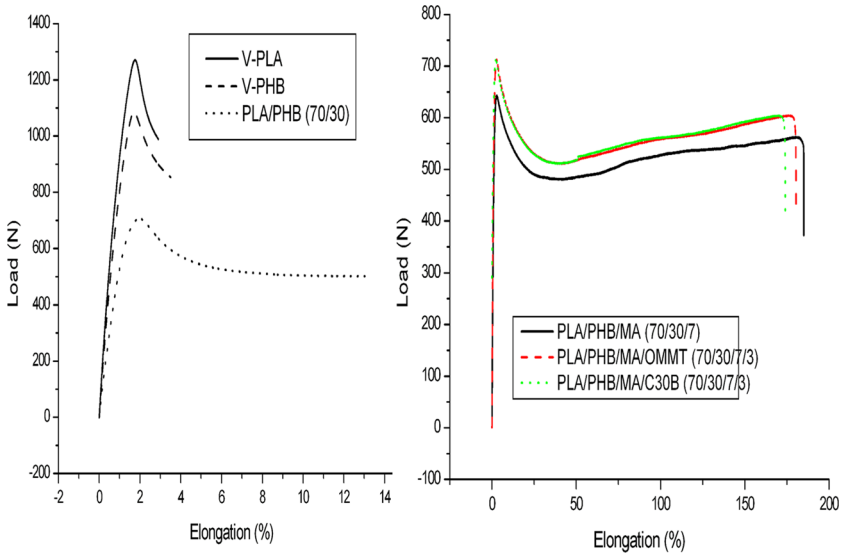

Figure 2. (a) Stress−strain curve of PLA, PHB, and PLA/PHB (70/30). (b) Stress−strain curve of PLA/PHB/MA (70/30/7) blend and its blend nanocomposites prepared from OMMT and C30B with 3 wt % nanoclay loading.

the blend matrix showed an increase to an optimum value of 540.17% with PLA/PHB/MA at a 70/30/7 ratio by wt %.

The same is demonstrated in the stress−strain curve depicted in Figure 2. As observed from the figure, V-PLA is very rigid, brittle, and showed a distinct yield point with subsequent failure immediately upon the tensile load. PLA/PHB (70/30) showed a continuous strain after distinct yielding with the stress remaining almost constant. The whitening phenomenon induced a large amount of craze during the tensile test. Extensive crazing of the blend resulted in larger strain at break and higher toughness than that of V-PLA. On the other hand, PLA/PHB/MA (70/30/7) showed initial strain softening after yielding and then underwent continuous cold drawing, which meant the necked down region prolonged under stress. The stress−strain curve beyond the yield point showed a combination of strain softening and cold drawing. This indicates that there was a competition between the PLA chain orientation and crack formation. Hence, a drop in stress with increasing strain has been observed. Beyond 100% of strain, a necking phenomenon appeared, and only cold drawing dominated at relatively constant stress. This phenomenon suggests that the main part of the fracture energy consumption has taken place due to making a plastic zone or stress whitening zone in front of the precrack. However, beyond 7 wt % of MA concentration, the blend matrix did not show any appreciable increase in elongation at break, which is probably due to the presence of an excess amount of MA that contributes in slippage of chains, thereby reducing the properties.

A similar increase in impact strength was also noticed with the incorporation of a MA compatibilizer. The notched impact strength of V-PLA increased to 49.2 J/m in the case of the PLA/PHB blend with 7 wt % of MA concentration. The result is around 99% higher than that of V-PLA, which further reveals the compatibilization of PLA and PHB with MA. However, enhanced ductility further reduced the stiffness of PLA/PHB blends after MA compatibilization. The blends displayed a consistent decrease in tensile strength and tensile modulus as depicted in the table. This can be explained through the expected phenomenon of replacement of stiffer bonds with flexible dipole−dipole and hydrogen bonding by MA bridging that tends to reduce the rigidity by distorting the crystalline arrangement of the matrix. The compatibilized blend at 7 wt % MA concentration was selected for nanocomposite preparation and further characterization.

Mechanical Properties of PLA/PHB Blend Nanocomposites. The addition of nanoclays to the compatibilized blend has resulted in positive results for the tensile modulus and tensile strength without compromising their higher ductility character. Both blend nanocomposites showed a similar range of increment in tensile modulus and tensile strength with an increased amount of nanoclays. C30B nanoclay loading up to 3 wt % showed a continuous increase in tensile strength and tensile modulus to 33.64 and 4222.64 MPa, respectively. These values are 49% and 5% better than those of the corresponding compatibilized blend. On the other hand, blend nanocomposites prepared using OMMT nanoclay exhibited better results with optimum values of tensile strength of 38.23 MPa and tensile modulus of 4332.56 MPa at 3 wt % nanoclay content. Increases of 69.5% and 7.7% in tensile strength and tensile modulus, respectively, have been observed as compared with the corresponding compatibilized blend. The increment in tensile modulus and tensile strength is mainly attributed to the nucleating characteristics of well-dispersed nanoclay layers that enhance the percentage of crystallinity within the blend matrix.[9] The increased crystallinity enhances the stiffness of the matrix thereby increasing the tensile strength and tensile modulus. HTAB modification of natural montmorillonite results in expansion of basal spacing from 1.3 to 3.1 nm. This allows easy penetration of polymer macromolecules into the interstitial spaces of silicate layers, which leads to well intercalated/exfoliated nanoclays within the matrix. On the other hand, the hydroxylated organomodifier ends on the C30B layers establish strong interfacial interactions with the carbonyl groups present in both the PLA and PHB macromolecules, which result in better mechanical properties for the blend nanocomposite. However, above 3 wt % of nanoclay loading, both of the blend nanocomposites have shown deterioration in mechanical properties, which may be due to the agglomeration of nanoparticles at this higher loading.

The percentage of elongation in the blend nanocomposites has shown a decrease as compared to the compatibilized blend due to its increased stiffness. A 3% loading of C30B and OMMT within the compatibilized blend has been reported and 457% and 488% elongations at break, respectively. However, the values are still significantly greater than that of the elongation of V-PLA, even though the impact strength was increased further and reported at 57.74 and 59.65 J/m, respectively, for C30B- and OMMT-reinforced blend nanocomposites. On the basis of the overall mechanical properties of the blend nanocomposites, the composition with 3% loading of both nanoclays has been opted for further characterization.

Morphology of PLA/PHB Blends and Blend Nanocomposites. *Evaluation of Miscibility of the PLA/PHB Blend Using FT-IR and SEM.* A comparative evaluation of miscibility of the PLA/PHB (70/30) blend and MA-compatibilized PLA/PHB (70/30/7) blend has been conducted here. Miscibility of blends notably depends upon the composition and molecular weight of the individual components. Figure 3(a,b) shows the

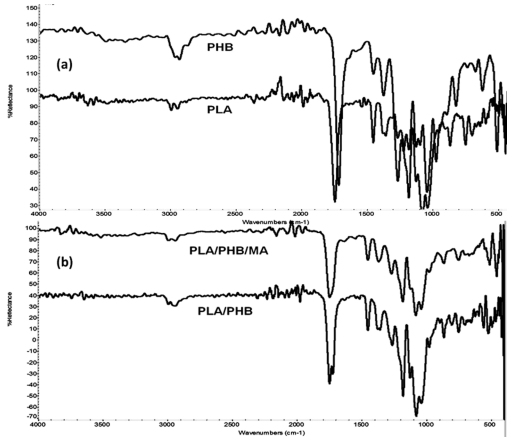

Figure 3. (a) FT-IR spectra of PLA and PHB. (b) FT-IR spectra of uncompatibilized and MA-compatibilized blends.

FT-IR spectra of V-PLA, V-PHB, PLA/PHB (70/30), and PLA/PHB/MA (70/30/7). All characteristics peaks like δ(C−O−C) at 1181 cm^{-1}, δ(C−O) at 1127 cm^{-1}, δ(C−H) at 2973 cm^{-1}, and δ(C═O) at 1747 cm^{-1} hve been identified for PLA material. Similarly, the PHB matrix also exhibited FT-IR spectra of identical functional groups at comparable stretching and bending frequencies as in PLA, which is depicted in Figure 3(a). An additional stretching frequency around 2980 cm^{-1} of C−H for CH_3 was observed in the case of the PHB material.

Several studies reported that the miscibility of the polymer blends can be evaluated appropriately by monitoring the changes in IR vibrational frequency of the C═O group. In such studies, high sensitivity of the C═O functional group on the crystallinity part of the polymeric materials has been utilized for the evaluation of miscibility. In the present study, a semicrystalline PLA with a δ(C═O) of 1747 cm^{-1} has been blended with another semicrystalline polymer of PHB with a δ(C═O) of 1714 cm^{-1}. The weak interaction between the carbonyl groups and hydrogen atoms of both the matrices through dipole−dipole and hydrogen bonding leads to a partially miscible blend, which results in an overlaid C═O peak around 1727 cm^{-1} in the FT-IR spectra of the PLA/PHB blend as depicted in Figure 3(b). Carbonyl groups in the PLA and PHB macromolecules can induce a partial polar nature to the C−H bonds located at their α and β positions. The resulting $H^{\delta+}$, can network with $O^{\delta+}$ of the carbonyl groups of other macromolecules through intra- and inter-molecular hydrogen bonding which in turn reduces the difference in peak position for C═O of PLA and PHB. This is evident from the FT-IR spectra of the PLA/PHB blend wherein an overlaid peak for C═O stretching at a lower crystallinity region than that of PLA was observed.

Further, the compatibilized blend using MA showed a single sharp peak around 1725 cm^{-1} for C═O stretching, which indicates uniformity in the vibrational frequencies of the functional group by MA bridges. As shown in Figure 1(a), grafting of MA occurs through the substitution reaction of α hydrogen atoms of carbonyl groups from both the matrices. The decrease in intensity of the peak around 2990 cm^{-1} corresponds to δ(C−H), which indicates successful grafting of MA on the matrices. MA grafting has been further confirmed by the absence of pure anhydride, the δ(C═O) peak in the spectra of the PLA/PHB/MA blend. However, the intermolecular 3D network structure created by the grafted MA restricts various C═O functionalities present in both polymers to a uniform vibrational frequency. The presence of such interactions result in better miscibility in the blend, and this has been proven by the sharp single peak around 1725 cm^{-1} for carbonyl groups (C═O) in the FT-IR spectra of PLA/PHB/MA.

The above depicted assumptions of increased miscibility by MA grafting are further supported with SEM images depicted in Figure 4(a−c). The SEM image of the tensile fractured surface

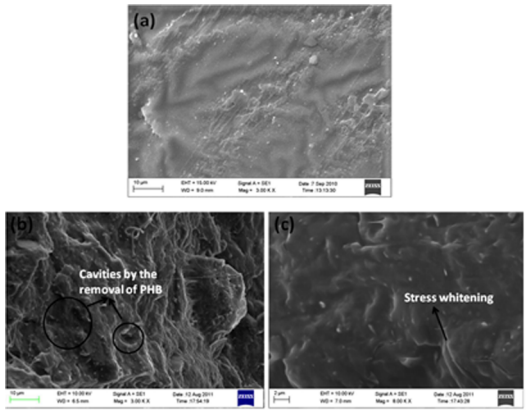

Figure 4. SEM images of (a) PLA, (b) PLA/PHB(70/30), and (c) PLA/PHB/MA(70/30/7).

of V-PLA (Figure 4(a)) is extremely flat and smooth, indicating brittle fracture of PLA under tensile loading. On the other hand, the PLA/PHB blend matrix displayed a relatively rough surface, which lacked ductile tearing and showed traces of phase-separated morphology as depicted in Figure 4(b). Formation of large voids was considered as the coalescence of neighboring small cavities caused by PHB debonding from the PLA matrix. The big voids not only resulted in a severe decrease in strength but also induced cracks, which finally triggered catastrophic failure under tensile loading. Conversely, highly ordered ligaments and lowered phase separation and roughness appeared on the tensile fractured surface of the PLA/PHB/MA blend (Figure 4(c)). This revealed improved compatibility in between the two matrices as a result of MA grafting and suggested that the failure mode changed from

dx.doi.org/10.1021/sc400395s | ACS Sustainable Chem. Eng. 2014, 2, 377−386

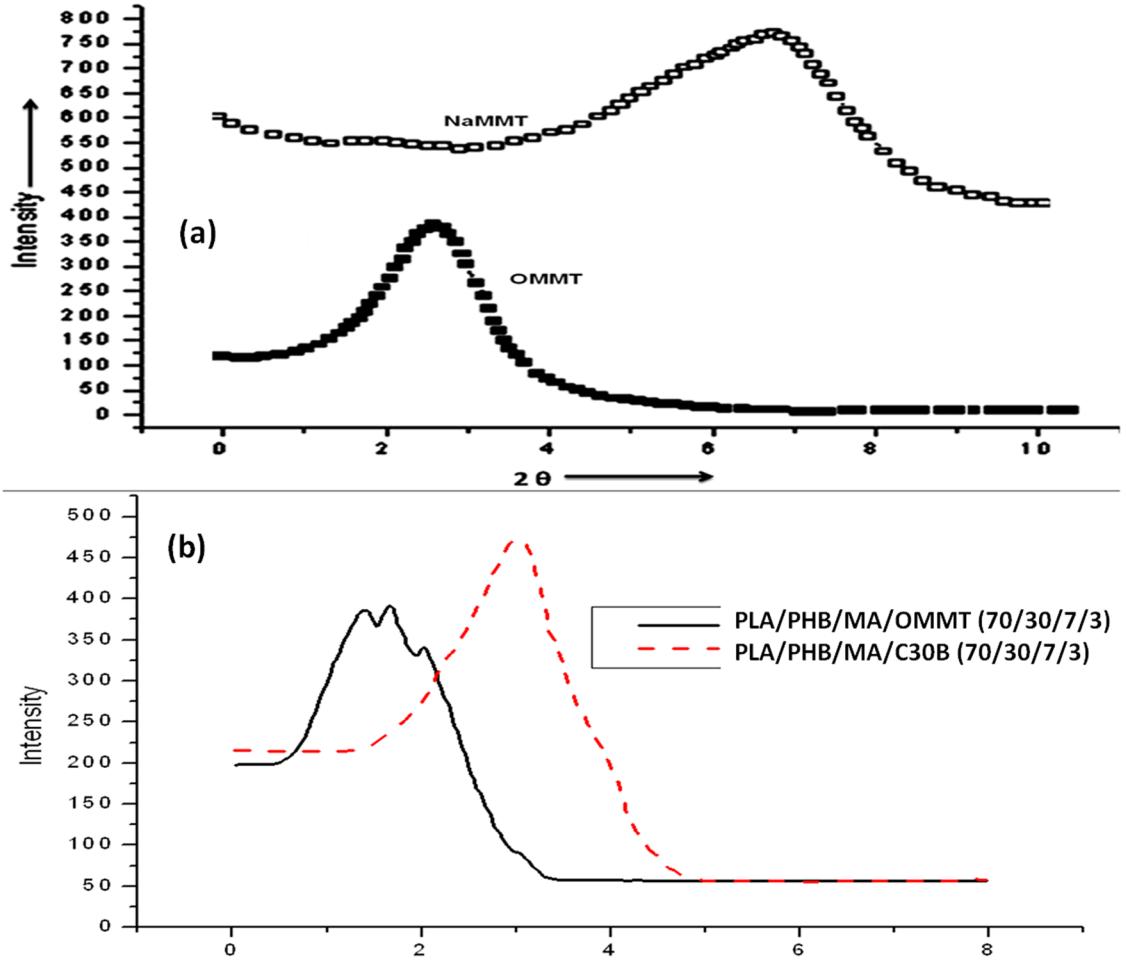

Figure 5. (a) WAXD pattern for virgin nanoclays. (b) Blend nanocomposites prepared from OMMT and C30B.

brittle fracture to ductile. Beside this stress, whitening ligaments revealed that the crack propagation absorbed considerable strain energy before failure.

Morphological Analysis of Blend Nanocomposites Using WAXD and TEM. Figure 5 represents the WAXD patterns of OMMT and blend nanocomposites prepared from OMMT and C30B. The (001) ordered diffraction of OMMT nanoclay was observed at $2\theta = 2.62°$ corresponding to a basal spacing of 3.1 nm. In the case of PLA/PHB/MA/OMMT blend nanocomposites, a number of peaks with increased d spacing of 4, 4.9, and 5.4 nm revealed a mixed morphology of intercalated and exfoliated nanoclays. Corresponding 2θ values were reported for (001) and its higher order diffractions (002) and (003) at 2.16°, 1.72°, and 1.48° respectively. On the other hand, the blend matrix with the C30B nanoclay exhibited a single sharp peak at $2\theta = 3.1°$ with d spacing of 3.5 nm, thus revealing typical characteristics of intercalated morphology. The pristine C30B nanoclay has a characteristic 2θ value at 4.78° with corresponding d spacing of 1.85 nm. It is assumed that the methyl hydrogenated tallow bis(2-hydroxy ethyl) ammonium modifier of C30B establishes a strong interaction of the PLA/PHB blend thus providing easy exfoliation/intercalation of the silicate layers.

TEM images of the PLA/PHB/OMMT and PLA/PHB/C30B blend nanocomposites are depicted in Figure 6(a,b), respectively. The gray areas represent the nanoclays, whereas the bright areas indicate the matrix polymers. As observed from

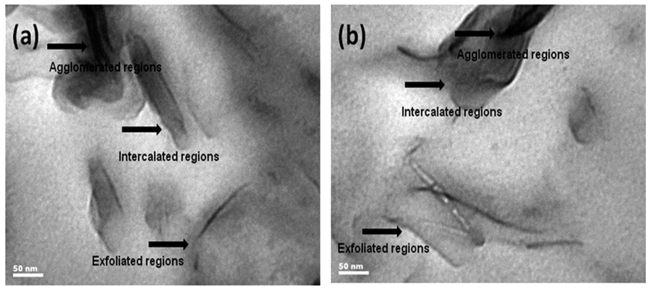

Figure 6. TEM images of blend nanocomposites prepared from (a) OMMT and (b) C30B.

the figure, both nanocomposites show a mixed morphology with the coexistence of exfoliated and intercalated clay patterns within the blend matrix. The observed morphology further suggests the effective reinforcing effect of both nanoclays within the blend matrix. Proper shear under optimized processing temperature, rpm, and retention time, along with effectively higher basal spacing and interacting groups present in the nanoclays facilitate easy penetration of polymer macromolecules into the nanoclay and its platelets dislocation. However, in both cases, few regions of stacks with agglomerated clay galleries were noticed.

Thermal properties. *DSC Analysis of PLA/PHB Blend and Blend Nanocomposites.* DSC thermograms from a second heating scan of V-PLA, V-PHB, blends, and blend nano-

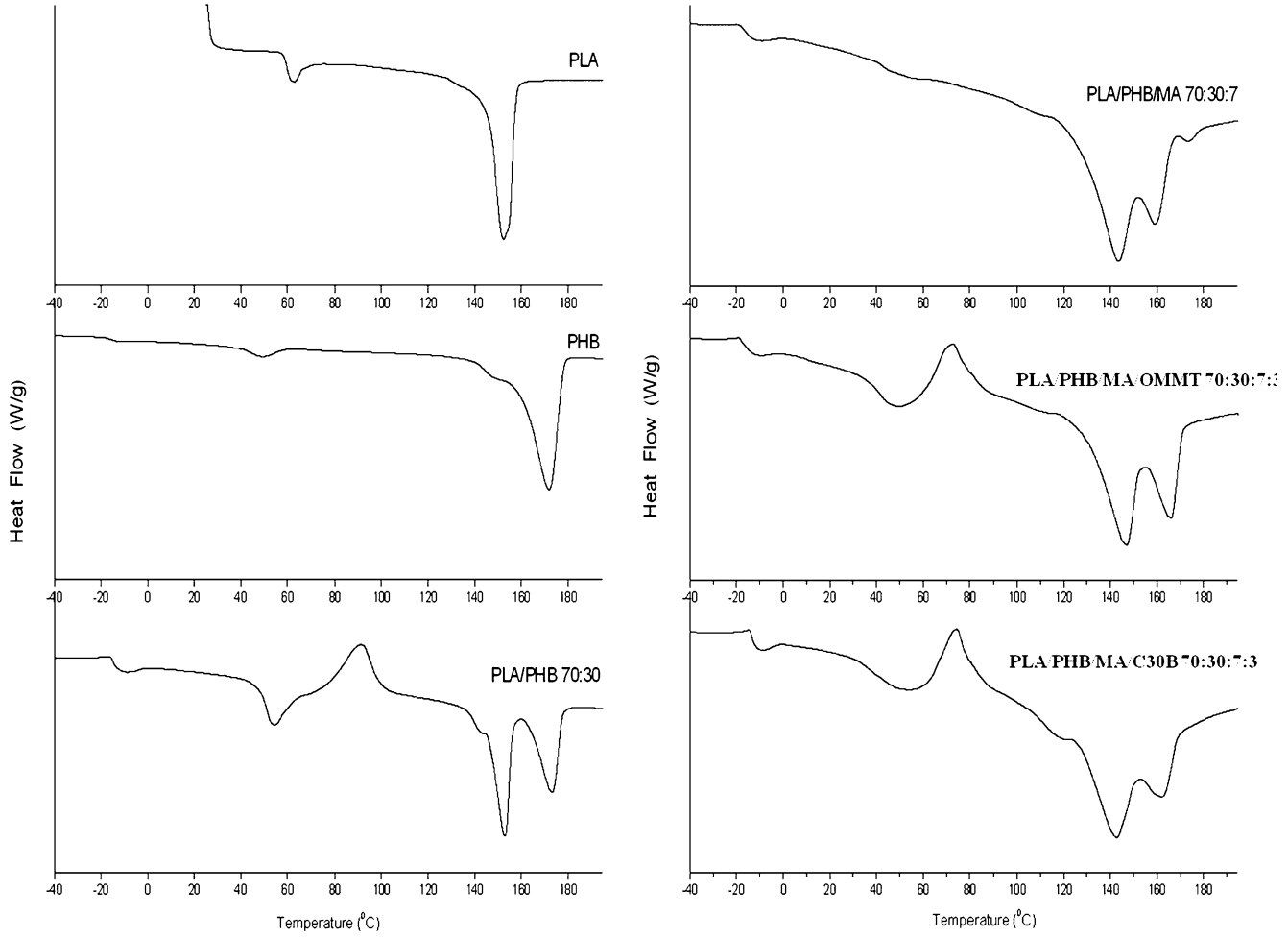

Figure 7. DSC thermograms of PLA, PHB, blends, and blend nanocomposites.

composites are depicted in Figure 7. The thermograms consist of transitions corresponding to three different regions forming successively during the heating cycle of DSC analysis: glass transition (T_g), cold crystallization (T_{cc}), and melting transition (T_m).

Evaluation of Miscibility of Blends Using T_g from DSC Analysis. Comparison of T_g of individual polymers in virgin form and in the blend is an effective tool to study the extent of miscibility in a partially miscible blend. V-PHB showed a T_g at −16.5 °C with V-PLA at 57.3 °C. In the PLA/PHB blends, T_g values corresponding to PHB shifted to −15 °C, which is 1.5 °C higher than the T_g of V-PHB. This reveals that PHB crystals act as fillers, immobilizing the PLA chains. On the other hand, the T_g of PLA dramatically reduced to 52.3 °C, which is further based on the assumption that PHB perhaps acts like a particular/elastomer, which contributes in lowering the T_g of PLA. However, the presence of two T_g corresponding to individual polymers reveals typical characteristics of partially miscible blends. Further, with the addition of MA and nanoclays, the difference in T_g of both PLA and PHB in the blend matrix reduces, which indicates an enhanced degree of interaction between the two matrices through a dipole−dipole interaction and hydrogen bonding. In the case of the MA-compatibilized PLA/PHB blend, T_g corresponding to the PHB matrix was noticed at −13.5 °C and for PLA at 42.7 °C. The difference in T_g corresponding to both matrices reduces to 58 °C in the blend, which indicated increased miscibility as a result of MA grafting. This difference is around 20 °C less than that observed in the case of virgin matrices.

The experimental observations have been further confirmed theoretically using the Flory−Huggins (F−H) theory

$$\Delta G/RTV = (\varphi_1/N_1)\ln \varphi_1 + (\varphi_2/N_2)\ln \varphi_2 + \chi_{12}\varphi_1\varphi_2$$

where ΔG is the change in free energy of mixing, R is the universal gas constant, V is the total volume of mixing, φ_1 and φ_2 are the volume fractions of PLA and PHB, respectively, and N_1 and N_2 are molar volumes of PLA and PHB, respectively. χ_{12} is the Flory interaction parameters, which can be determined using following equation

$$\chi_{12} = (\delta_1 - \delta_2)^2/RT > 0$$

$[\delta_1-\delta_2]$ is the difference in solubility parameters and if χ_{12} is less than zero ($\chi_{12} < 0$), the blend is considered as completely miscible in nature.

ΔG has been calculated using the F−H equation and is in good agreement with the ΔG obtained from the enthalpy of mixing of the PLA/PHB blend. The theoretically calculated and experimentally determined ΔG values have been found to be 3.2 and 3.7 KJ/mol, respectively. A small positive ΔG for the blend indicates partial miscibility between high molecular weight PLA and PHB, whereas a miscible blend supposedly gives a negative ΔG. On the other hand, the ΔG of mixing for the PLA/PHB/MA blend is found to be 2.2 KJ/mol and that of the calculated value using the F−H equation is 2.37 KJ/mol.

dx.doi.org/10.1021/sc400395s | ACS Sustainable Chem. Eng. 2014, 2, 377−386

The reduced ΔG value indicates increased feasibility of the process due to the additional physical interactions created by MA compatibilization. The F−H interaction parameter calculated has been found to be 3.67×10^{-3}, a much lower positive value, which also suggests a partially miscible blend between higher molecular weight PLA and PHB.

However, in the case of PLA/PHB/MA/C30B and PLA/PHB/MA/OMMT blend nanocomposites, the T_g values corresponding to PLA increased marginally as compared with the compatibilized blend PLA/PHB/MA. PLA/PHB/MA/C30B showed T_g values at −12.4 and 43.7 °C, corresponding to the PHB and PLA segments, respectively. On the other hand, PLA/PHB/MA/OMMT exhibited optimum T_g at −11.3 and 44.2 °C, similar to the above-mentioned order. This fact reveals that the nanoclays (OMMT and C30B) act as reinforcing agents and are preferentially distributed in PLA, restricting its mobility at the interface of the blend.

V-PLA displayed a cold crystallization exotherm at 114.4 °C. On the other hand, V-PHB did not show any T_{cc} peak. Comparing, the exothermic peak of V-PLA, the blends and blend nanocomposites showed better crystallization characteristics with lower T_{cc}. The PLA/PHB blend showed T_{cc} at 113.2 °C, which is further reduced to 92.4 °C by the compatibilization process using MA. The T_{cc} peaks observed for both blends are narrowed and are lower in area in comparison with V-PLA. This indicates the fact that although the blend has increased crystallizability, the total crystallanity of PLA has been reduced by melt blending with PHB and MA. This phenomenon is well supported by lower ΔH_{cc} and ΔH_m values obtained for the blend systems as compared with V-PLA. PLA is a slow crystallizing material, which needs a wide frame of crystallization time for the molecular rearrangements. Th presence of flexible physical interactions tends to reduce the crystallinity but facilitates easy crystallization of the remaining crystalline domain through additional physical interactions. Compatibilization using MA creates better physical interactions within the blend interface, hence resulting in lower T_{cc} than that of the blend without a compatibilizer. However, the addition of organically modified nanoclays tends to enhance the crystallizabillity as well as the crystallinity of blends significantly. The C30B-reinforced blend nanocomposite showed T_{cc} at 82.4 °C, whereas its OMMT counterpart cold crystallizes at 75.4 °C as a result of the nucleating capability of nanoclays within the PLA/PHB/MA blend. Increased ΔH_{cc} and ΔH_m in the case of blend nanocomposites also underline the above observations. However, in the present study, T_{cc} has been considered instead of T_c to detect the crystallization in PLA. Hence, the phenomenon of recrystallization has not been taken into account.

V-PLA showed T_m at 148.6 °C with a broad shoulder whereas, V-PHB showed a sharp melting peak at 172.0 °C. The PLA/PHB blend without MA exhibited a typical double melting transition of a partially miscible blend with distinct peaks at 146.2 and 163.4 °C corresponding to PLA and PHB, respectively. The peak corresponding to PLA was also associated with a discrete shoulder corresponding to the melting of crystals with different geometries formed during the cold crystallization process. However, the T_m values reduced considerably in comparison with the virgin materials, indicating some decrease in miscibility. Further, with the incorporation of MA, the T_m of individual matrices exhibit balanced transitions with the peak drawing closer to each other. Mohanty et al. also reported similar phenomenon of the lowering of the melt temperature of PHB by MA grafting.[10] According to the author, the toughening effect of PHB-g-MA in relation with the flexible hydrogen bond interlocking may tend to reduce the melting point of the material. On the contrary, incorporation of organically modified nanoclays, OMMT and C30B, increases the T_m of both PLA and PHB in the blend, which can be explained by similar reinforcement effects of the nanoclays. Further, as observed in the earlier sections, the double melting characteristics of PLA also could not be noticed in the presence of PHB and MA.

Thermogravimetric Analysis (TGA). Thermal stability of V-PLA, V-PHB, PLA/PHB blends, and blend nanocomposites are depicted in Figure 8. V-PLA showed a single-step degradation pattern with an initial (T_i) and maximum degradation temperature (T_{max}) of 251.3 and 327.4 °C, respectively. On the other hand, V-PHB revealed the onset degradation temperature T_i at 223.4 °C, which shows that PLA has higher thermal stability as compared with that of PHB. However, thermal degradation of the PLA/PHB blend displayed a two-step degradation attributed to both matrices but at higher temperature regions as expected from the interaction between the polar functionalities in the blend. The blend matrix exhibited two major degradation temperatures at 270.8 and 325.4 °C, respectively. The initial temperature corresponds to the degradation of the PHB segment, and the second degradation temperature corresponds to PLA. However, the MA-incorporated blend showed a marginally enhanced T_{max} to 270.4 and 326.5 °C, corresponding to the degradation of PHB and PLA, respectively.

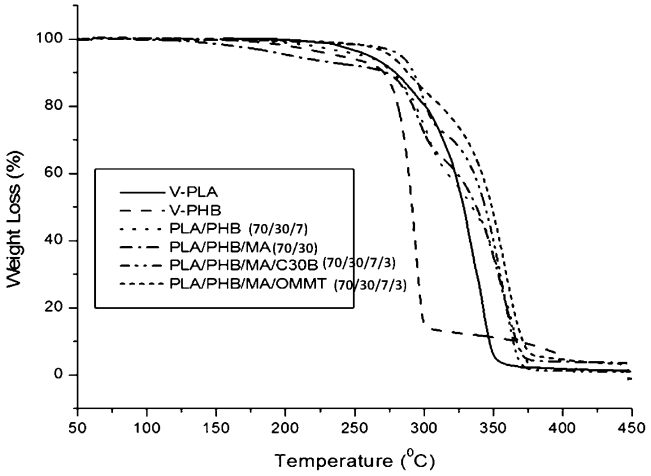

Figure 8. Thermal stability of PLA, PHB, blends, and blend nanocomposites.

Conversely, both blend nanocomposites exhibited improved thermal stability as compared with the compatibilized and uncompatibilized blend matrix. Incorporation of C30B and OMMT nanoclays within the blend resulted in an increase in the degradation of PHB and PLA to 277.5 and 280.1 °C. The increase in thermal degradation temperature by incorporating nanoclays can be attributed to a decrease in O_2 permeability due to the so-called "tortuous path" effect of the filler.[11] This phenomenon delays the permeation of oxygen and the escape of volatile degradation products. Also, the inorganic fillers like layered silicates improve the char formation during thermal degradation. Both blend nanocomposites showed around a 4% residue formation after the maximum degradation temper-

atures, which also underline the increased thermal stability for PLA and the compatibilized blend after reinforcement with nanoclays. In addition to this, there may be thermodynamic factors such as an increase in the activation energy of thermal degradation in the polymer nanocomposites. In the present investigation, the effects have supported in a pronounced way the case of using OMMT-reinforced blend nanocomposites. The observation again supports a better level of exfoliation/intercalation of OMMT within the compatibilized blend.

Dynamic Mechanical Analysis. Figure 9(a) represents the storage modulus virgin matrices, blends, and blend nano-

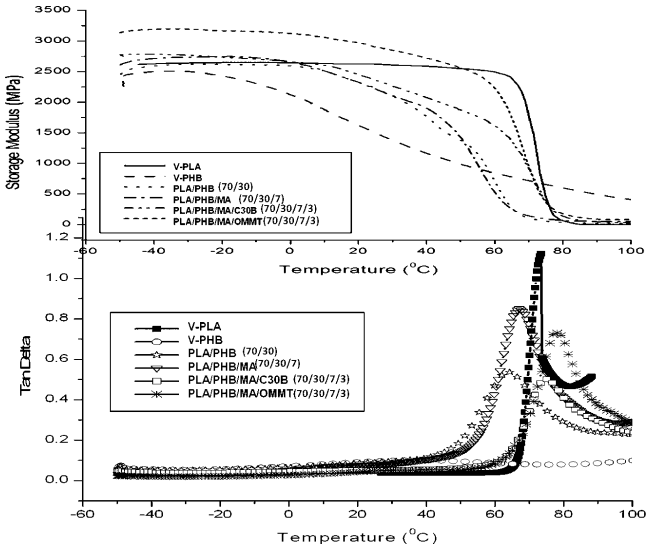

Figure 9. DMA analysis of PLA, PHB, PLA/PHB blends, and blend nanocomposites.

composites. Apart from the V-PHB, all samples, including V-PLA, displayed three different regions for storage modulus curves. In the case of V-PLA, a stable plateau was observed until the T_g around 67 °C, before the modulus, decreased drastically due to the macromolecular relaxation in the rubbery region, followed by another stable plateau up to 100 °C. On the other hand, V-PHB exhibited a plateau region until the T_g region of the matrix around −20 °C, beyond the modulus, dropped continuously until 100 °C due to the chain relaxation process. Further, the PLA/PHB (with and without MA) blend and blend nanocomposites followed a multi-step chain relaxation process displaying a stable plateau until 15−20 °C, which probably corresponds to the T_g of the PHB matrix. The blend nanocomposites displayed a higher T_g, corresponding to the PHB along with the broadening of the transition region, thus confirming segmental immobilization of PLA chains due to the presence of PHB crystals. Also it is evident that the blend nanocomposites with C30B display a higher magnitude of E′ than both V-PLA and V-PHB withinthe range from −50 to 20 °C. In thecase of the PLA/PHB/MA/C30B blend nanocomposite, the rate of fall of the matrix modulus is compensated by the presence of C30B, which is clearly observed from the increase in E′, beyond T_g of PHB at 18 °C and that of PLA at 60 °C, as compared with the blend. On the contrary, the blend nanocomposite prepared using the OMMT nanoclay depicted higher E′ as compared with all the samples over the investigated range of temperature from −50 to 65 °C. However, beyond 65 °C, corresponding to the T_g of PLA, the modulus falls and is less than V-PLA, which is possibly due to the presence of PHB. This further confirms the improved interfacial balance in the PLA/PHB/MA/OMMT blend nanocomposite.

As evident from the tan δ curve (Figure 9(b)), V-PHB displayed a broadened transition region with a minimum magnitude of tan δ. V-PLA revealed a relaxation maximum around 75 °C in the tan δ curve, which subsequently increased in both blend nanocomposites. The C30B-reinforced blend nanocomposite exhibited a marginal increase to 77.5 °C, which is probably because C30B has a polar hydroxylated organic end that bonds strongly with the matrix polymer though physical interaction. However, the nanocomposite prepared using the OMMT nanoclay showed an optimum increase in the relaxation maximum to 81 °C, thus indicating improved dispersion characteristics of the organically modified nanoclay with the blend matrix as explained in an earlier section. On the contrary, the blends with and without MA displayed a lower value of T_g, which is possibly due to the incompatibility at the interface. In all of the cases, the T_g corresponding PHB could not be detected; hence, only the values corresponding to PLA have been reported.

CONCLUSIONS

Compatibilized blends of PLA and PHB using MA have been prepared successfully under optimized processing conditions. Characterization studies have proven that MA can be used as an effective compatibilizer for the PLA/PHB blend. Further, the reduced stiffness of the PLA by blending and compatibilization has been compensated by reinforcing nanoclays C30B and OMMT. FT-IR sensitivity on the variation in crystallinity through carbonyl stretching studies, SEM images, and a comparative study of T_g of the blends with virgin materials confirms the increased miscibility by MA coupling within the PLA/PHB blend. Further, mechanical properties propose well-toughened blends and blend nanocomposites after the incorporation of the reactive compatibilizer. Final blend nanocomposites have been given increased tensile properties in terms of tensile modulus (above 4200 MPa), tensile strength (above 43 MPa), elongation at break (above 450%), and impact strength (above 57 J/m), which are significantly higher than those of V-PLA. In addition, dynamic mechanical analysis also proposed positive effect reactive compatibilization and nanoclay reinforcement in terms of increased storage modulus and tan δ values. Thermal stability also was reported at a higher range for PLA as a function of nanoclay reinforcement. In the present study, OMMT-reinforced PLA/PHB/MA blend nanocomposites have recorded superior performance characteristics, such as mechanical, thermal, and morphological properties, compared to those of its C30B counterpart.

AUTHOR INFORMATION

Corresponding Author

*E-mail: larpmcipet@gmail.com. Phone: 0674 2742852.

Notes

The authors declare no competing financial interest.

REFERENCES

(1) Hongzhi, L.; Jinwen, Z. Research, progress in toughening modification of poly(lactic acid). *J. Polym. Sci., Part B: Polym. Phys.* **2011**, *49*, 15.

(2) Ohkoshi, I.; Abe, H.; Doi, Y. Miscibility and solid-state structures for blends of poly((S)-lactide) with atactic poly((R,S)-3-hydroxybutyrate). *Polymer* **2000**, *41*, 5985.

(3) Koyama, N.; Doi, Y. Miscibility of binary blends of poly[(R)-3-hydroxybutyric acid] and poly[(S)-lactic acid]. *Polymer* **1997**, *38*, 1589.
(4) Yu, L.; Dean, K.; Li, L. Polymer blends and composites from renewable resources. *Prog. Polym. Sci.* **2006**, *31* (6), 576.
(5) Zhang, L.; Xiong, C.; Deng, X. Miscibility, crystallization and morphology of poly(b-hydroxybutyrate)/poly(D,L-lactide). *Polymer.* **1996**, *37*, 235.
(6) Jandas, P. J.; Mohanty, S.; Nayak, S. K. Rheological and mechanical characterization of renewable resource based high molecular weight PLA nanocomposites. *J. Polym.* **2013**, DOI: 10.1155/2013/403467.
(7) Kumar, M.; Mohanty, S.; Nayak, S. K.; Rahail, P. M. Effect of glycidyl methacrylate (GMA) on the thermal, mechanical and morphological property of biodegradable PLA/PBAT blend and its nanocomposites. *Bioresour. Technol.* **2010**, *101* (21), 8406.
(8) Gedde, U. L. F. *Polymer Physics*; Kluwer Acadamic Publishers: The Netherlands, 2001.
(9) Jandas, P. J.; Mohanty, S.; Nayak, S. K. High molecular PLA based natural fiber reinforce nanocomposites for disposable applications. *J. Clean. Prod.* **2013**, *52* (1), 392.
(10) Mohanty, A. K. Anhydride Functionalized Polyhydroxyalkanoates, preparation and use thereof. U.S. Patent 2005/0215672 A1.
(11) Okamoto, M. *Polymer/Clay Nanocomposites: Encyclopedia of Nanoscience and Nanotechnology*; American Scientific Publishers: Stevenson Ranch, CA, 2004.